Research article

Inhibition of β2-adrenergic receptor regulates necroptosis in prostate cancer cell

Shiqi Wu [1], Meixi Li [1], Fangfang Chen, Yan Zeng, Chen Xu [*,1]

Institution of Life Science, Chongqing Medical University, Chongqing, China

ARTICLE INFO

ABSTRACT

As the malignant tumor with the highest incidence in male, prostate cancer poses a significant threat to the reproductive health of elderly men. Our previous studies have shown that promoting necroptosis of cancer cells can effectively inhibit cancer cell proliferation. This study includes lentivirus-mediated knockdown of β2AR which resulted in stable transfectants that exhibited an increased ability to form clones compared to that of the negative control group. In the protein and mRNA levels, necroptosis associated RIP and mixed lineage kinase domain-like (MLKL) were significantly higher in the treatment group than they were in the control group. Furthermore, cells treated with propranolol exhibited necrotic morphology as observed by transmission electron microscopy. The combination of β2AR suppression and necroptosis inhibitors resulted in a more potent suppression of cell proliferation compared to that observed in the control and negative control groups. Additionally, it elevated in the necrosis rate as determined by flow cytometry. Immunofluorescence staining revealed enhanced RIP and MLKL expression in the sh-β2AR group compared to levels in the negative control group. Co-immunoprecipitation experiments detected an interaction between β2AR and RIP. MLKL and RIPK3 levels were significantly higher in xenograft tumor sections from the sh-β2AR group compared to levels in the sh-NC group. To conclude, our research indicates the proliferation of PC-3 and DU-145 cprostate cancer cells can be suppressed by inhibiting β2AR, and this occurs through the RIP/MLKL-mediated pathway of necroptosis.

1. Introduction

Prostate cancer is the predominant malignant neoplasm affecting males worldwide [1,2]. Extensive studies have confirmed the role of the autonomic nervous system [3] in regulating prostate cancer cell growth and metastasis [4]. Previous studies have demonstrated considerable suppression of cancer cell growth and promotion of cell death by using inhibitors of the β2AR [5] or by reducing the expression of β2AR. Historically, necrosis has been considered to be an uncontrollable [6–9] (β2AR) and unplanned method of cell death. β2AR regulates different types of cell death, including non-programmed and programmed, it has been supported by literatures that β2AR can regulate apoptosis [10,11], pyroptosis and autophagy [12] in various cancer cells.

Historically, necrosis has been seen as an uncontrollable [13], non-planned way of cell death. In 2005, Degterev et al. [14] first

---

Abbreviations	
β2AR	β2 adrenergic receptor
Nec-1	necrostatin-1
RIP	receptor-interacting protein
MLKL	mixed lineage kinase domain-like
PRO	Propranolol

presented the idea of necroptosis, a unique form of cellular death that cannot be stopped by general caspase inhibitors but can be inhibited explicitly by necrostatin-1(Nec-1). Necroptosis shares morphological characteristics with necrosis, including compromised cell membrane integrity and nuclear dissolution; however, it is genetically regulated. The main components of the necroptotic pathway are RIP [15] and MLKL [16,17]proteins. Feng, X et al. have reported that necroptosis suppresses colorectal cancer [18]. Furthermore, deficiency of RIP in breast tumor cells had been testified that it was positively selected during tumor development and growth [19].

However, it remains unclear whether β2AR inhibits or promotes the progression of prostate cancer cell. We aim to investigate the anti-tumor effects of β2AR inhibition and examine its mechanisms linked to necroptosis.

2. Materials and methods

2.1. Regents

The culture medium (DMEM/F12) was purchased from Gbico(NY, USA). Fetal bovine serum was provided by Biological Industries (Kibbutz Beit Haemek, Israel). SP-0023 immunohistochemistry and DAB staining kits were purchased from ZSGB (Beijing, China). Propranolol hydrochloride (PRO), necrostatin-1 (Nec-1), Rabbit anti-β2AR, anti-RIP antibody and Protein A/G immunoprecipitation magnetic beads were obtained from Selleck (Selleck Chemicals, Houston, USA). The TSZ(C1058S) method for inducing cell necroptosis, penicillin-streptomycin solution, rabbit IgG, and WB and IP lysis buffers were obtained from Beyotime (Beyotime Institute of Technology, Beijing, China). The antibodies against RIPK3 and MLKL were obtained from Abcam (Cambridge, MA, USA). Tsingke (Beijing, China) provided the RT-PCR primers Table 1, while Shanghai Genechem (China) conducted the β2AR RNAi and lentivirus packaging.

2.2. Cell culture

Human prostate cancer cells The PCa cell lines PC-3(RRID: CVCL_0035) and DU-145(RRID: CVCL_0105) were obtained from the Shanghai Institute of Life Sciences (Shanghai, CHINA). The cell lines were authenticated by Prcella STR profiling, and all experiments were performed with mycoplasma-free cells. Prostate PC-3 and DU-145 cells were grown in DMEM/F12 medium containing 10 % fetal bovine serum at 37 °C in an environment with 5 % CO_2 and saturated humidity. Subsequent experiments used cells in the logarithmic growth phase. The study was separated into control and Pro treatment groups (150 μmol/L for 24, 48, and 72 h).

2.3. Lentiviral infection

In a six-well plate, PC-3 and DU-145 cells (1×10^5 cells/well) were distributed and then separated into two groups that included the negative control group (transfected with negative control) and the sh-β2AR group (transfected with β2AR-RNAi). Each group comprised three replicates. Upon reaching 40–50 % confluence, the cells were transfected according to the guidelines provided by the lentivirus transfection kit. After 12 h, the medium was replaced with a fresh complete medium to continue the culture. Passage culture was performed 72 h after transfection, and puromycin (15 μg/mL) was used for stable cell clone selection.

2.4. Cell proliferation assay

PC3 and DU-145 cells (3×10^3 cells/well) were seeded into 96-well plates. Following a 24-h incubation period, cells were subjected to various doses of Pro (ranging from 50 to 250 μmol/L) for 24, 48, or 72 h. Next, the culture medium was substituted, and each well

Table 1
Sequences of primers for RT-PCR

Genes	Primers	
RIPK1	Forward	TTACATGGAAAAGGCGTGATACA
	Reverse	AGGTCTGCGATCTTAATGTGGA
MLKL	Forward	GACCAAGGAAAGAGGAGCGT
	Reverse	GCTTCCTGTTCACGTCCTTG
β-Actin	Forward	CGGCACCACCATGTACCCT
	Forward	ACACGGAGTACTTGCGCTCAG

received 90 μL of medium along with 10 μL of CCK-8 solution. Cell viability was determined by measuring the absorbance at 450 nm (A) after incubating at 37 °C for 1–4 h. Cell viability (%) was calculated as (A of experimental well - A of blank well)/(A of control well - A of blank well) *100 %. GraphPad Prism 9 software calculates the IC_{50} (half-maximal inhibitory concentration).

2.5. Cell clone formation assay

A six-well plate was used to seed the cell suspensions at a density of 500 cells per well. Following cell attachment, wells were treated with varying concentrations (0 and 150 μmol/L) of Pro for 72 h. Then, the medium was then replaced, and the cells were incubated for 14 days. When visible clones appeared in the wells, the culture was terminated. The liquid was discarded and treated with 4 % polyformaldehyde solution for 30 min. After removing the fixative, 5 % crystal violet staining solution was added for 10–30 min. After washing with phosphate buffered solution (PBS), the plates were imaged on a white surface. ImageJ software was used to quantify the colony retina, and statistical analysis was conducted using GraphPad Prism 9 software.

2.6. Flow cytometry for PI/Annexin V-FITC

A six-well plate was used to seed cells at a density of 1×10^5 cells per well. Following treatment, cells were collected, rinsed twice with PBS, and transferred to flow tubes. Centrifugation was performed on the tubes at a temperature of 4 °C and a speed of 1000 rpm for 5 min, and the supernatant was then removed. The final solution contains the isolated cells, and 1 mL of PBS and 5 μL of Annexin V-FITC was introduced. Following a 15-min incubation in a dimly lit environment at ambient temperature, 5 μL of PI was added and thoroughly mixed in the dark for 5 min, and the reaction was then detected by flow cytometric analysis.

2.7. Western blot

Cells were seeded into a six-well dish at 1×10^5 cells per well. Following various procedures, the cells were lysed in Radio Immunoprecipitation Assay (RIPA) lysis buffer to extract the total proteins. A BCA assay was used to determine protein concentration. The gels for electrophoresis and transfer were prepared according to the procedures for 10 % SDS-PAGE. Antibodies against RIP, MLKL, and β2AR were added at a dilution of 1:1,000, and incubation was performed overnight at 4 °C. Next, the proteins were exposed to a 1:50,000 dilution of goat anti-rabbit secondary antibody or a 1:5000 dilution of goat anti-mouse secondary antibody for 1h at RT. An ECL chemiluminescence system was used to develop the membranes in the ChemiDoc imaging system.

2.8. Real-time fluorescent quantitative PCR

The concentration was measured after extracting the total RNA using an RNA extraction kit. The RNA was converted to cDNA by reverse transcription using a reverse transcription kit. SYBR reagent (5 μL), F/R primers (0.2 μL each), DEPC water (3.6 μL), and cDNA (1 μL) were mixed and added to the reaction. The conditions for real-time PCR included initial denaturation at 95 °C for 5 min that was followed by 41 amplification cycles (10 s at 95 °C, 30 s at 58 °C, and 20 s at 72 °C). The Bio-Rad CFX Maestro software was used to analyze the results.

2.9. Transmission electron microscopy

Cells were seeded into culture dishes (6 cm). Following treatment, the cells were collected and spun in 15 mL centrifuge tubes at 800 rpm for 5 min. Next, the liquid was removed, and the cells were resuspended in 1 mL of PBS. They were centrifuged in 1.5 mL Eppendorf tubes at 1200 rpm for 10 min. A solution of glutaraldehyde at a concentration of 2.5 % was carefully introduced along the inner surface of the tube for overnight fixation. After treatment with 1 % osmium tetroxide for 2 h, the specimens were dehydrated in ethanol and acetone. Subsequently, they were infiltrated with epoxy resin 812, embedded, polymerized, and sectioned. After staining with uranyl acetate and lead citrate, the sections were examined using a JEOL JEM-1400PLUS transmission electron microscope.

2.10. Immunofluorescence staining

A total of 2×10^4 cells per well were plated into 24-well plates with coverslips. Following this procedure, the cells were rinsed with PBS, treated with 4 % paraformaldehyde for 20 min, and subsequently washed three times with PBS for 5 min per wash. The cells were then incubated in permeabilization buffer for 15 min at room temperature. For blocking, 5 % goat serum was used for 1 h, and the primary antibody (1:200) against the target protein was then incubated overnight at 4 °C. Using an appropriately diluted fluorescent secondary antibody, cells were gently shaken in the dark for 1 h after washing with PBS. Nuclear staining was performed by adding DAPI for 5 min, and this was followed by rinsing with PBS. After retrieving and mounting the coverslips, the cells were observed under a fluorescence microscope.

2.11. CO-immunoprecipitation

The cells were distributed into sh-NC and sh-β2AR groups after being plated in 10 cm culture dishes. WB and IP lysis buffers containing protease inhibitors were used for protein extraction to obtain total proteins. The input group (whole cell lysate) consisted of

100 μL of supernatant mixed with 25 μL of 5 × SDS loading buffer that was then boiled at 95 °C for 10 min. The IP group (target protein group) consisted of 400 μL of supernatant mixed with anti-RIPK3 (rabbit) antibody, while the IgG group consisted of 200 μL of supernatant mixed with the same amount of anti-IgG (rabbit). Both groups were incubated overnight in a rotator at 4 °C. After pretreatment, the protein A/G magnetic beads were introduced to the protein-antibody compound that had undergone overnight incubation at 4 °C. The mixture was then placed on a rotator at the same temperature for 2 h. The beads were washed five times with a cold wash buffer to remove the supernatant. Next, the beads were combined with an equivalent amount of 1 × loading buffer, heated at 95 °C for 10 min, and examined by western blotting. The antibody dilutions included rabbit anti-RIPK3, β2AR antibody (1:1000) and rabbit anti-human GAPDH polyclonal antibody (1:2000).

2.12. Immunohistochemical staining of subcutaneous tumors in nude mice

One million shNC and shβ2-AR shRNA cells of PC-3 were suspended in phosphate-buffered saline and injected into one subaxilla of each 4-week-old male BALB/c-nude mouse (HFK Bio, China) to generate xenografts. Tumor tissues from the animal experiments (sh-NC and sh-β2AR groups) were embedded and sectioned. The segments were placed in a 60 °C oven for 1 h, deparaffinized, and subsequently transferred to sodium citrate buffer for antigen retrieval by subjecting them to intense heat for 5 min followed by mild heat for 20 min. Endogenous peroxidases were removed by heating. After rinsing with phosphate buffered saline (PBS), the sections were blocked with 10 % goat serum for 30 min. The primary antibodies that included RIPK3 and MLKL (1:50) were added and left to incubate overnight at 4 °C. The following day, the sections were incubated at ambient temperature for 30 min, rinsed with PBS, and
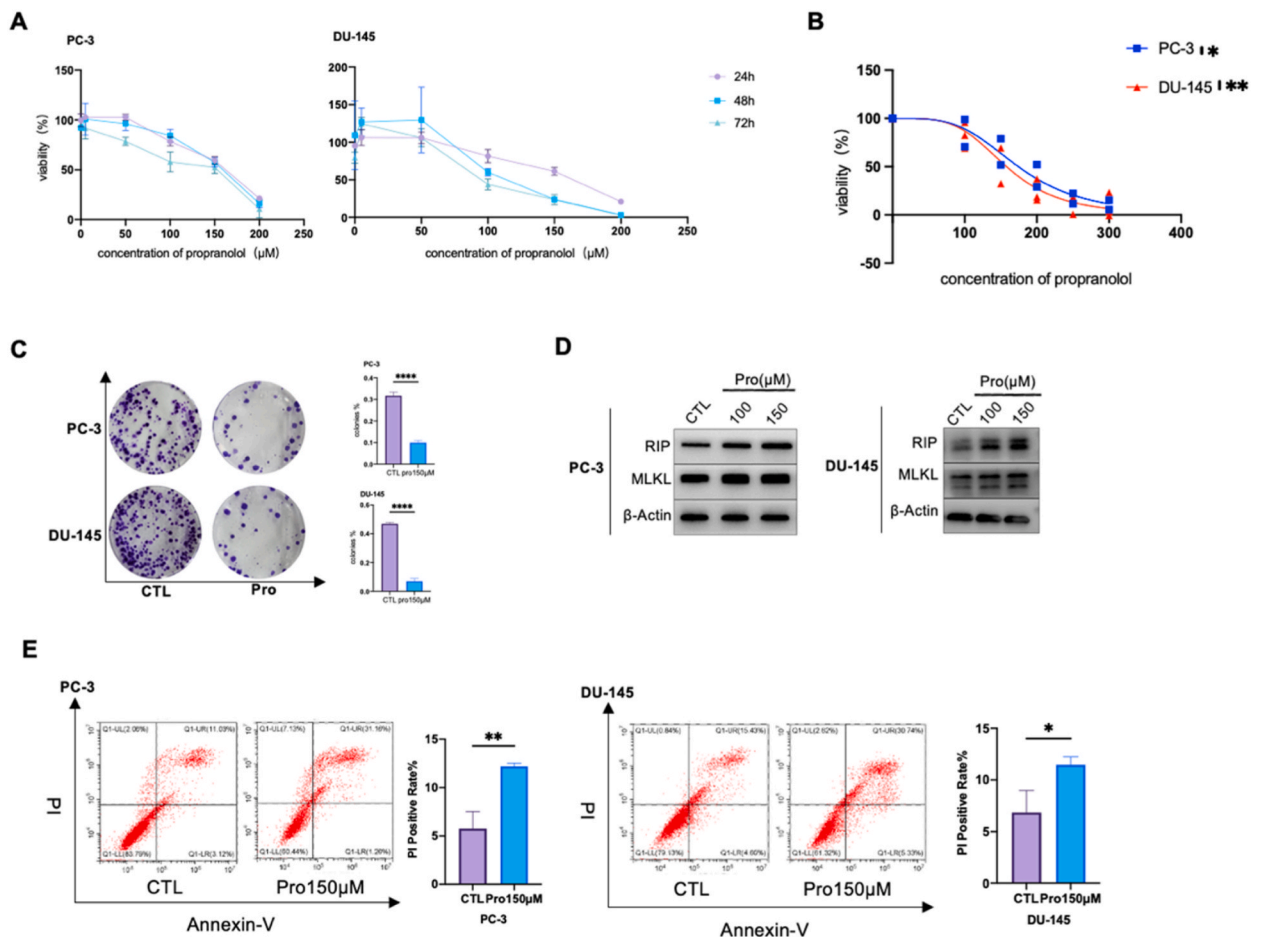

Fig. 1. The effects of propranolol on the viability, proliferation, and protein expression in PC-3 and DU-145 cells. A. Using the CCK-8 assay determined the survival rate of PC-3 and DU-145 cells exposed to different concentrations and durations of propranolol. B. The CCK-8 assay measured the IC50 values of PC-3 and DU-145 cells after being treated with various concentrations of propranolol for 72 h. C. The ability of PC-3 and DU-145 cells to form colonies was significantly decreased when treated with 150 μM propranolol, compared to the control group (P < 0.01). D. The expression levels of RIP and MLKL proteins were increased in PC-3 and DU-145 cells when treated with propranolol at concentrations of 100 and 150 μM, in comparison to the control group. Full, non-adjusted gels were include in Figure Supplementary materials. E. Treatment using 150 μM propranolol led to a significant rise in the PI-positive rate of PC-3 and DU-145 cells (P < 0.05). Each data represents the mean of three independent experiments (n = 3). P-value was calculated by Student's t-test. *p < 0.05, **p < 0.01,****p < 0.0001.

treated with goat anti-rabbit IgG. The segments were then cultured in a working solution labeled with horseradish peroxidase. After the PBS washes, the sections were treated with DAB, rinsed with flowing water to eliminate any extra staining, and finally counterstained with hematoxylin. Afterwards, the segments were dehydrated, clarified, air-dried, and mounted. Three fields were examined and photographed to determine the number of positive cells in each section. To determine the percentage of positive cells, the number of positive cells was divided by the total cell count and multiplied by 100.

2.13. Statistical analysis

Statistical analyses were performed Using GraphPad Prism 9 software. Comparisons between two groups were conducted using an
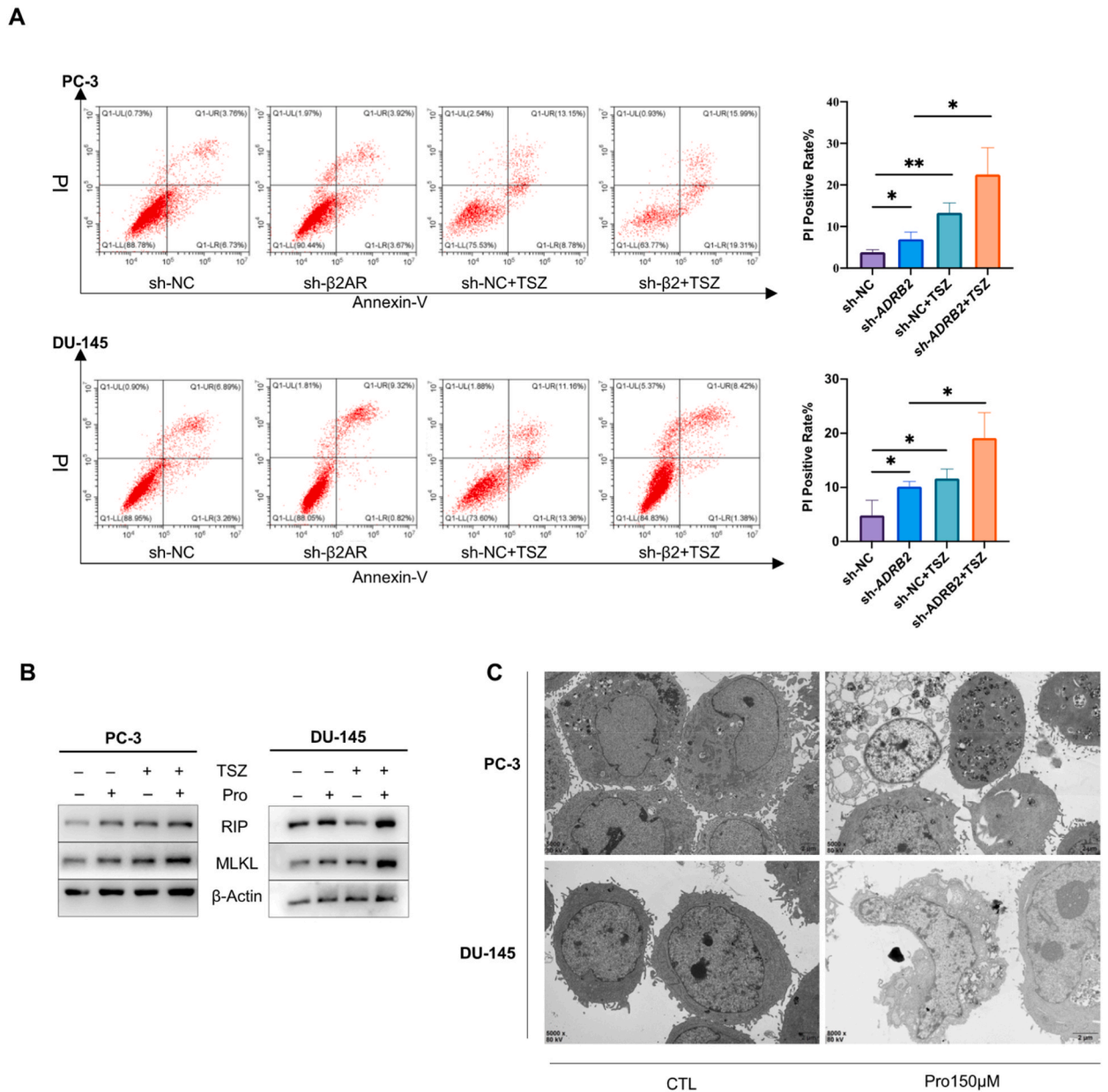

Fig. 2. Necroptosis in PC-3 and DU-145 cells was reduced by inhibiting or suppressing β2AR. A. Knocking down β2AR led to necroptosis, which caused a significantly greater number of PI-positive cells (indicating necrosis) compared to the control group (P < 0.05). B. Compared to the control group, the expression levels of RIP and MLKL proteins in PC-3 and DU-145 cells were elevated by suppression of β2AR and additional stimulation of necroptosis. Full, non-adjusted gels were include in Figure Supplementary materials. C. After β2AR inhibition (PRO treated), cells displayed distinct signs of necrosis, including membrane rupture, swelling, and dissolution. All data was presented as mean ± SD from three independent experiments and calculated by Student's *t*-test. Error bars represent SD. *p < 0.05, **p < 0.01.β-Actin was used as a loading control in Fig2B.

independent sample *t*-test. Comparisons among multiple groups were conducted using one-way analysis of variance (ANOVA). The significance level was set at p = 0.05.

3. Results

3.1. Reducing or suppressing the effect of β2AR on the activity and growth rate of PC-3 and DU-145 cells

The results obtained from the CCK-8 test suggest that the survival rate of PC-3 and DU-145 cells decreased in a dose- and time-dependent manner after treatment with propranolol at concentrations of 50, 100, 150, 200, and 250 μmol/L for 24, 48, to 72 h (P < 0.05, Fig. 1A). Significant disparities in cell viability were observed at various concentrations of propranolol at 24, 48, and 72 h. The IC_{50} values for PC-3 and DU-145 cells after 72 h were observed to be 174.4 μmol/L (with a 95 % confidence interval of 152.6–196.1 μmol/L) and 158.1 μmol/L (with a 95 % confidence interval of 140.4–175.2 μmol/L), respectively (P < 0.05, Fig. 1B). Based on these results, the subsequent experiments opted for the administration of propranolol at a concentration of 150 μmol/L for 72 h.

The colony formation assay results revealed a substantial decrease in clone formation rate in PC-3 and DU-145 cells that were treated with 150 μmol/L of PRO compared to the control group (P < 0.01, Fig. 1C).

3.2. When β2AR expression is inhibited or suppressed, there is a significant rise in the rate of cell necroptosis, which is further enhanced when combined with the necroptosis inducer TSZ

To establish stable transgenic clones with reduced β2AR expression, β2AR RNAi lentivirus was used to infect PC-3 and DU-145 cells.
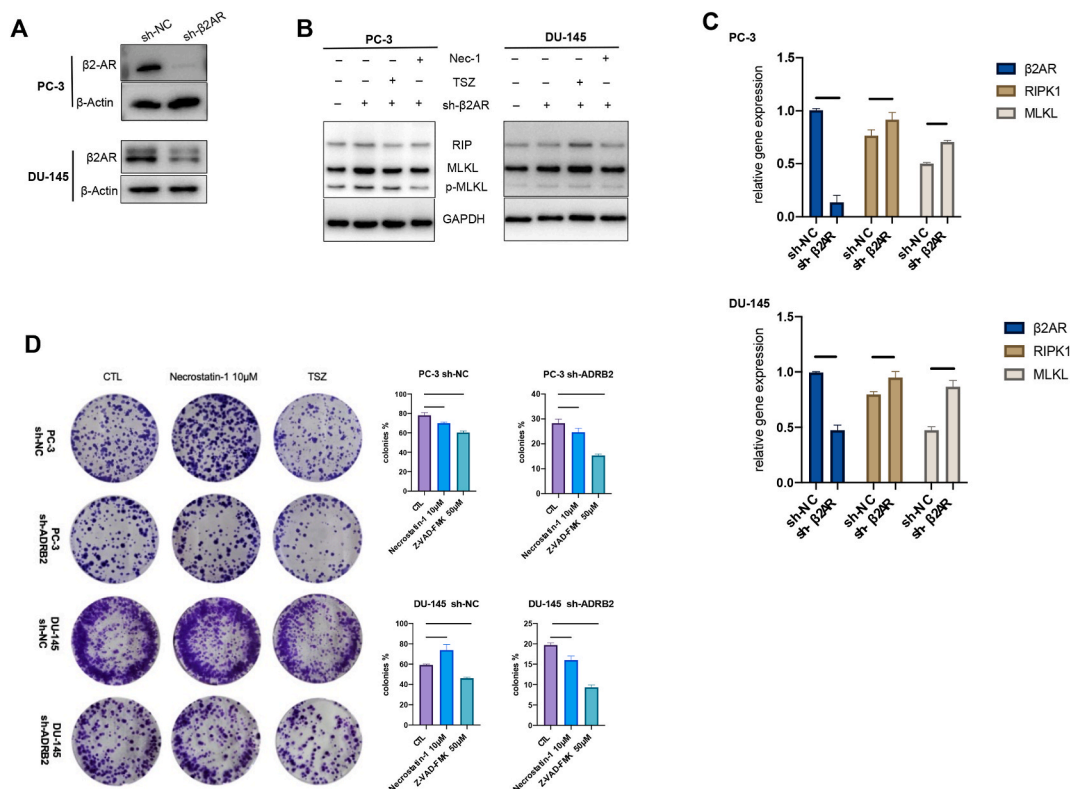

Fig. 3. The impact on cell proliferation and the expression of mRNA and proteins related to necroptosis, with suppression of β2AR and the induction or inhibition of necroptosis. A.β2AR protein expression levels in PC-3 and DU-145 cells following a knockdown. Full, non-adjusted gels were include in Figure Supplementary materials. B. The knockdown of β2AR resulted in an elevation of necrosis-related protein expression specific to the cells. Concurrent blocking of β2AR and stimulation of necroptosis led to elevated levels of RIP and MLKL protein expression. The expression levels of RIP and MLKL proteins remained unchanged in cells treated with both β2AR inhibition and necroptosis induction, as compared to the NC group. C. Knocking down β2AR resulted in elevated levels of cell-specific mRNA expression linked to necrosis (P < 0.05). D. Knockdown of β2AR decreased the colony formation rate. The colony formation rate was further reduced when β2AR inhibition was combined with necroptosis induction in comparison to the control group. Concurrent suppression of β2AR and necroptosis led to a reduction in cellular proliferation ability in comparison to the control cohort. All data was presented as mean ± SD from three independent experiments and calculated by Student's *t*-test. Error bars represent SD. *p < 0.05, **p < 0.01, ***p < 0.001, ****p < 0.0001. β-Actin was used as a loading control in Fig3A.GAPDH was used as a loading control in Fig3B.

The sh-β2AR group exhibited a marked decrease in the levels of β2AR mRNA as determined by RT-PCR analysis compared to levels in the negative control (NC) group (P < 0.01, Fig. 3C). The Western blot analysis demonstrated a notable reduction in levels of β2AR protein in the sh-β2AR group compared to levels in the NC group (P < 0.01, as shown in Fig. 3A). The results indicate that the β2AR gene was effectively suppressed in the cancer cells, thus demonstrating evidence of successful knockdown.

In the colony formation experiment, cells with decreased β2AR expression exhibited a notable decline in clone formation rate in comparison to that of the control group. This effect was more pronounced when combined with the necroptosis inducer TSZ. In contrast, the use of the necroptosis suppressant Nec-1 along with TSZ resulted in an increase in the rate (P < 0.05, Fig. 3D).

The effects of treating prostate cancer cell lines with 150 μmol/L of propranolol (Fig. 1E) and sh-β2AR knockdown (Fig. 2A) were evaluated using flow cytometry analysis. Necrosis identification involved Annexin V-FITC and PI dual staining. These findings demonstrated a notable increase in the proportion of PI-positive cells in both experimental cohorts, thus suggesting the occurrence of necrosis. Moreover, necrosis was notably diminished in cells undergoing sh-β2AR knockdown after necroptosis induction, thus indicating a significant influence on the necrosis rate.

3.3. Inhibition or knockdown of β2AR promotes the expression of RIP and MLKL, subsequently inducing necroptosis

After administering propranolol or suppressing β2AR in the two cell lines, we observed an increase in MLKL and RIP (P < 0.05, Fig. 3C), both of which are acknowledged indicators of necroptosis. There was a notable increase in RIPK1 and MLKL mRNA levels. The cells possessed increased levels of MLKL and RIP when β2AR was inhibited (Fig. 1D) or knockdown was performed as revealed by Western blot analysis (Fig. 3B). Moreover, the addition of the TSZ necroptosis stimulant further increased the levels of MLKL and RIP proteins (Figs. 2B and 3B). However, the simultaneous suppression of β2AR and the necroptosis inhibitor Nec-1 did not result in a reduction in the levels of MLKL and RIP proteins (Fig. 3B).

Further immunofluorescence experiments revealed a consistent trend of RIPK3 and MLKL protein changes (Figs. 4 and 5).

3.4. Necrotic alterations occur when β2AR is inhibited in PC-3 and DU-145 cells

Transmission electron microscopy demonstrated analysis that following propranolol treatment, the majority of cells in both cell lines displayed characteristic morphological indications of cell necrosis such as cell membrane rupture, cytoplasmic vacuole formation, nuclear condensation, fragmentation, and dissolution (Fig. 2C).

3.5. Interaction of β2AR and the necroptosis-specific protein

Co-IP and Western blot analysis revealed the presence of β2AR and the necroptosis-specific protein RIPK3 in PC-3 and DU-145 cells and also indicated their interaction. Nevertheless, there were no notable alterations that were observed in the interaction between
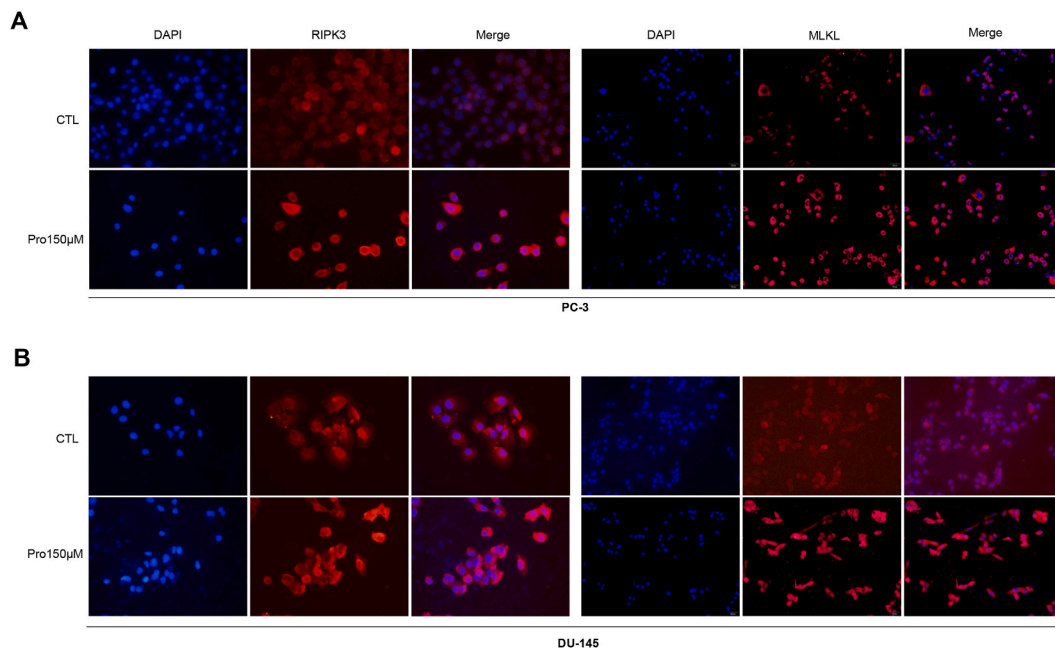

Fig. 4. The levels of RIPK3 and MLKL expression in control and PRO treated groups. A. Fluorescence intensity were considerably elevated in PC-3 cells when blocking β2AR led to a notable rise in the levels of RIPK3 and MLKL expression versus the control group. B. Fluorescence intensity was detected in DU-145 cells as PC-3 cells.
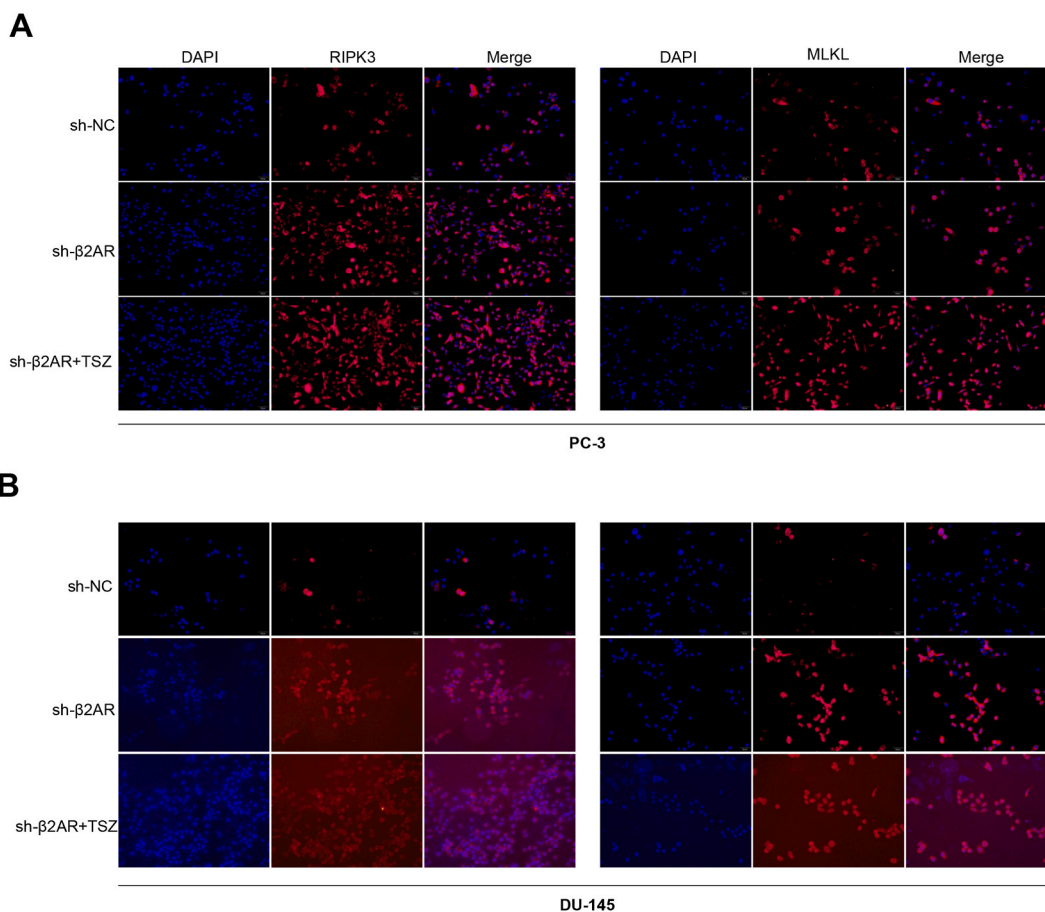
A

PC-3

B

DU-145

Fig. 5. The levels of RIPK3 and MLKL expression in NC and sh groups. A. Fluorescence intensity were considerably elevated in PC-3 cells when β2AR was suppressed and/or necroptosis was induced, in comparison to the sh-NC group. B. Fluorescence intensity was detected in DU-145 cells as PC-3 above TSZ refers to necroptosis inducer drug.

β2AR and RIPK3 following β2AR depletion (Fig. 6A).

3.6. Immunohistochemistry revealed significant expression of RIPK3 and MLKL in sh-β2AR xenografts of prostate cancer

We performed immunohistochemical analysis and detected the expression of necroptosis associated markers in xenograft tissues, in xenograft tumors derived from β2-AR knockdown cells of PC-3, we found significant upregulations of RIPK3 and MLKL (P < 0.05, Fig. 6B).

4. Discussion

The autonomic nervous system has been observed to exert a considerable impact on the development and progression [20]of prostate cancer. Studies have demonstrated a significant increase in sympathetic nerve activity [21,22]n tissues linked to high-risk prostate cancer, with β2AR [6,7,23,24] playing a vital role in the sympathetic nervous system signaling pathway. The analysis of the results revealed that patients who used propranolol for a long period of time experienced prolonged periods of survival [8,9,25,26]. Previous studies have also suggested that β2AR can augment the migratory and invasive abilities [27,28] of prostate cancer cells while also influencing cell death.

Necroptosis, a type of programmed cell death, differs from typical necrosis by its capacity to induce necroptosis via the control of specific genes and the classical RIP/MLKL pathway [29]. Necroptosis is initiated when RIPK3 [15] is activated by binding to RIPK1 [30] that then associates with its substrate MLKL [31]. Previous studies have confirmed the substantial participation of necroptosis in tumor progression [32], where suppressed necroptosis results in a particularly adverse prognosis for Acute myeloid leukemia (AML) [33], bladder cancer [34],and breast cancer [35]. The initiation of necroptosis is important for the treatment of ovarian cance [36] and colorectal carcinoma [37].

This study determined that the growth and multiplication of prostate cancer cells was significantly reduced by blocking β2AR with
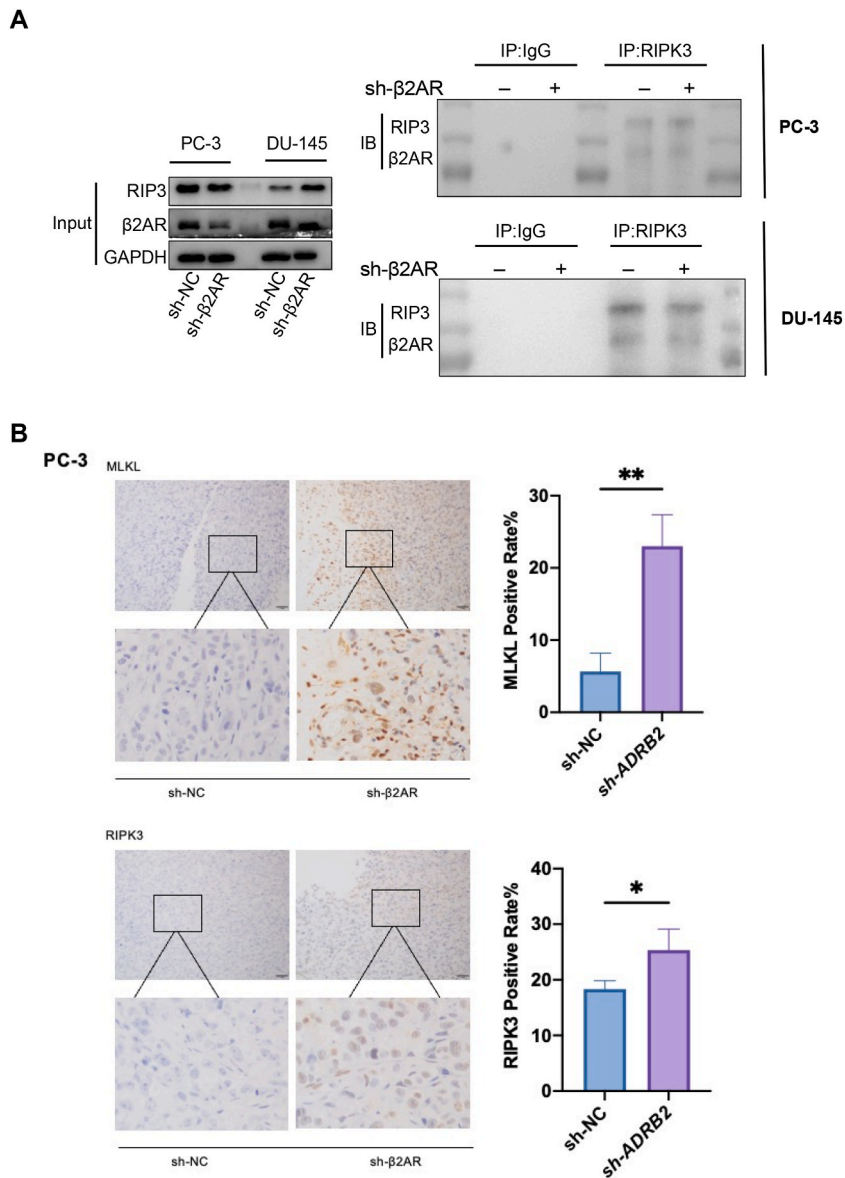
Fig. 6. Evidence for the interaction between β2AR and RIPK3 proteins. A. Proteins were obtained through co-immunoprecipitation experiments. The Input group was the cell lysate, as the positive control group, the IgG group was the protein similar to the target protein but did not bind, as the negative control group. The IP group is the protein of interest. Full, non-adjusted gels were include in Figure Supplementary materials. B. Furthermore, immunohistochemical analysis revealed that the depletion of β2AR resulted in an increase in the levels of RIPK3 and MLKL expression within the tissue. All data was presented as mean ± SD from three independent experiments and calculated by Student's *t*-test. Error bars represent SD. *p < 0.05, **p < 0.01. GAPDH was used as a loading control in Fig6A.

propranolol. Furthermore, this inhibitory effect was further suppressed in cells treated with a necroptosis inhibitor, whereas cell death was enhanced when a necrosis inducer was used. Propranolol treatment led to the identification of necrotic morphology in prostate cancer cells by transmission electron microscopy. Significantly, we determined that necroptosis was not induced by external physical factors and could be controlled by administering our drugs. Using flow cytometry, Annexin V-FITC and PI dual staining demonstrated a significant increase in the percentage of PI-positive cells in two types of prostate cancer cells when β2AR was inhibited or knocked down. This increase signified an increase in the rate of cell necrosis after treatment.

Moreover, the necroptosis markers RIP and MLKL were upregulated after treatment, and this could be counteracted by administering a necroptosis inhibitor (albeit without complete restoration to pre-drug application levels). However, the simultaneous suppression of β2AR and promotion of necroptosis resulted in a notable increase in the growth of prostate cancer cells. Our previous cell experiments align with the results of animal experiments, where the immunohistochemical staining of tumor tissues in nude mice revealed a significant increase in the expression levels of RIPK3 and MLKL after suppression of β2AR.

5. Conclusion

To summarize, our research has demonstrated that blocking β2AR can trigger necroptosis in prostate cancer, thus providing a more detailed understanding of the regulatory function of β2AR in prostate cancer. Moreover, our discoveries indicate the possible use of propranolol, a blocker of β2AR, for the medical treatment of cancer. However, the regulation of necroptosis involves various pathways, thus necessitating further research to elucidate the underlying mechanisms.

Funding

Ethics declarations

This study was reviewed and approved by The Ethics Committee of Chongqing Medical University, with the approval number: 2021092.

Data availability statement

Data included in article/supp. material/referenced in article.

CRediT authorship contribution statement

Shiqi Wu: Writing – review & editing, Writing – original draft, Methodology, Conceptualization. **Meixi Li:** Software, Methodology, Data curation. **Fangfang Chen:** Software, Project administration. **Yan Zeng:** Software, Methodology. **Chen Xu:** Visualization, Validation, Supervision, Resources, Project administration, Funding acquisition, Formal analysis, Data curation.

Declaration of competing interest

The authors declare that they have no known competing financial interests or personal relationships that could have appeared to influence the work reported in this paper.

Appendix A. Supplementary data

Supplementary data to this article can be found online at https://doi.org/10.1016/j.heliyon.2024.e31865.

References

[1] R.L. Siegel, K.D. Miller, N.S. Wagle, A. Jemal, Cancer statistics, CA Cancer J Clin 73 (2023) 17–48, https://doi.org/10.3322/caac.21763, 2023.
[2] H. Sung, J. Ferlay, R.L. Siegel, M. Laversanne, I. Soerjomataram, A. Jemal, F. Bray, Global cancer statistics 2020: GLOBOCAN estimates of incidence and mortality worldwide for 36 cancers in 185 countries, CA Cancer J Clin 71 (2021) 209–249, https://doi.org/10.3322/caac.21660.
[3] J.L. Mohler, E.S. Antonarakis, A.J. Armstrong, A.V. D'Amico, B.J. Davis, T. Dorff, J.A. Eastham, C.A. Enke, T.A. Farrington, C.S. Higano, E.M. Horwitz, M. Hurwitz, J.E. Ippolito, C.J. Kane, M.R. Kuettel, J.M. Lang, J. McKenney, G. Netto, D.F. Penson, E.R. Plimack, J.M. Pow-Sang, T.J. Pugh, S. Richey, M. Roach, S. Rosenfeld, E. Schaeffer, A. Shabsigh, E.J. Small, D.E. Spratt, S. Srinivas, J. Tward, D.A. Shead, D.A. Freedman-Cass, Prostate cancer, version 2.2019, JNCCN Journal of the National Comprehensive Cancer Network 17 (2019) 479–505, https://doi.org/10.6004/jnccn.2019.0023.
[4] A.H. Zahalka, A. Arnal-Estapé, M. Maryanovich, F. Nakahara, C.D. Cruz, L.W.S. Finley, P.S. Frenette, Adrenergic nerves activate an angio-metabolic switch in prostate cancer, Science (1979 358 (2017) 321–326, https://doi.org/10.1126/science.aah5072.
[5] D. Palm, K. Lang, B. Niggemann, T.L. Drell IV, K. Masur, K.S. Zaenker, F. Entschladen, The norepinephrine-driven metastasis development of PC-3 human prostate cancer cells in BALB/c nude mice is inhibited by β-blockers, Int. J. Cancer 118 (2006) 2744–2749, https://doi.org/10.1002/IJC.21723.
[6] Z. Huang, G. Li, Z. Zhang, R. Gu, W. Wang, X. Lai, Z.K. Cui, F. Zeng, S. Xu, F. Deng, β2AR-HIF-1α-CXCL12 signaling of osteoblasts activated by isoproterenol promotes migration and invasion of prostate cancer cells, BMC Cancer 19 (2019), https://doi.org/10.1186/S12885-019-6301-1.
[7] S. Hassan, A. Pullikuth, K.C. Nelson, A. Flores, Y. Karpova, D. Baiz, S. Zhu, G. Sui, Y. Huang, Y.A. Choi, R. D'Agostino, A. Hemal, U. von Holzen, W. Debinski, G. Kulik, β2-adrenoreceptor signaling increases therapy resistance in prostate cancer by upregulating MCL1, Mol. Cancer Res. 18 (2020) 1839–1848, https://doi.org/10.1158/1541-7786.MCR-19-1037.
[8] C.R. Cardwell, H.G. Coleman, L.J. Murray, J.M. O'Sullivan, D.G. Powe, Beta-blocker usage and prostate cancer survival: a nested case-control study in the UK Clinical Practice Research Datalink cohort, Cancer Epidemiol 38 (2014) 279–285, https://doi.org/10.1016/J.CANEP.2014.03.011.
[9] H.H. Grytli, M.W. Fagerland, K.A. Taskén, S.D. Fosså, L.L. Håheim, Use of β-blockers is associated with prostate cancer-specific survival in prostate cancer patients on androgen deprivation therapy, Prostate 73 (2013) 250–260, https://doi.org/10.1002/PROS.22564.
[10] M. Koh, T. Takahashi, Y. Kurokawa, T. Kobayashi, T. Saito, T. Ishida, S. Serada, M. Fujimoto, T. Naka, N. Wada, K. Yamashita, K. Tanaka, Y. Miyazaki, T. Makino, K. Nakajima, M. Yamasaki, H. Eguchi, Y. Doki, Propranolol suppresses gastric cancer cell growth by regulating proliferation and apoptosis, Gastric Cancer 24 (2021) 1037–1049, https://doi.org/10.1007/S10120-021-01184-7.
[11] J. Zhou, Z. Liu, L. Zhang, X. Hu, Z. Wang, H. Ni, Y. Wang, J. Qin, Activation of β2-adrenergic receptor promotes growth and angiogenesis in breast cancer by down-regulating PPARγ, Cancer Res Treat 52 (2020) 830–847, https://doi.org/10.4143/CRT.2019.510.
[12] M. Zhang, F. Chen, X. Sun, Y. Huang, Y. Zeng, J. Chen, S. Wu, C. Xu, Sympathetic β2-adrenergic receptor blockade overcomes docetaxel resistance in prostate cancer, Biochem. Biophys. Res. Commun. 657 (2023) 69–79, https://doi.org/10.1016/J.BBRC.2023.03.046.

[13] Z. Su, Z. Yang, Y. Xu, Y. Chen, Q. Yu, Apoptosis, autophagy, necroptosis, and cancer metastasis, Mol. Cancer 14 (2015), https://doi.org/10.1186/s12943-015-0321-5.

[14] A. Degterev, Z. Huang, M. Boyce, Y. Li, P. Jagtap, N. Mizushima, G.D. Cuny, T.J. Mitchison, M.A. Moskowitz, J. Yuan, Chemical inhibitor of nonapoptotic cell death with therapeutic potential for ischemic brain injury, Nat. Chem. Biol. 1 (2005) 112–119, https://doi.org/10.1038/nchembio711.

[15] S. He, L. Wang, L. Miao, T. Wang, F. Du, L. Zhao, X. Wang, Receptor interacting protein kinase-3 determines cellular necrotic response to TNF-α, Cell 137 (2009) 1100–1111, https://doi.org/10.1016/j.cell.2009.05.021.

[16] L. Sun, H. Wang, Z. Wang, S. He, S. Chen, D. Liao, L. Wang, J. Yan, W. Liu, X. Lei, X. Wang, Mixed lineage kinase domain-like protein mediates necrosis signaling downstream of RIP3 kinase, Cell 148 (2012) 213–227, https://doi.org/10.1016/j.cell.2011.11.031.

[17] H. Meng, Z. Liu, X. Li, H. Wang, T. Jin, G. Wu, B. Shan, D.E. Christofferson, C. Qi, Q. Yu, Y. Li, J. Yuan, Death-domain dimerization-mediated activation of RIPK1 controls necroptosis and RIPK1-dependent apoptosis, Proc Natl Acad Sci U S A 115 (2018) E2001–E2009, https://doi.org/10.1073/PNAS.1722013115.

[18] X. Feng, Q. Song, A. Yu, H. Tang, Z. Peng, X. Wang, Receptor-interacting protein kinase 3 is a predictor of survival and plays a tumor suppressive role in colorectal cancer, Neoplasma 62 (2015) 592–601, https://doi.org/10.4149/NEO_2015_071.

[19] G.B. Koo, M.J. Morgan, D.G. Lee, W.J. Kim, J.H. Yoon, J.S. Koo, S. Il Kim, S.J. Kim, M.K. Son, S.S. Hong, J.M.M. Levy, D.A. Pollyea, C.T. Jordan, P. Yan, D. Frankhouser, D. Nicolet, K. Maharry, G. Marcucci, K.S. Choi, H. Cho, A. Thorburn, Y.S. Kim, Methylation-dependent loss of RIP3 expression in cancer represses programmed necrosis in response to chemotherapeutics, Cell Res. 25 (2015) 707–725, https://doi.org/10.1038/CR.2015.56.

[20] H. Hondermarck, P. Jobling, The sympathetic nervous system drives tumor angiogenesis, Trends Cancer 4 (2018) 93–94, https://doi.org/10.1016/j.trecan.2017.11.008.

[21] S. Dwivedi, M. Bautista, S. Shrestha, H. Elhasasna, T. Chaphekar, F.S. Vizeacoumar, A. Krishnan, Sympathetic signaling facilitates progression of neuroendocrine prostate cancer, Cell Death Discov 7 (2021), https://doi.org/10.1038/S41420-021-00752-1.

[22] P.H. Thaker, L.Y. Han, A.A. Kamat, J.M. Arevalo, R. Takahashi, C. Lu, N.B. Jennings, G. Armaiz-Pena, J.A. Bankson, M. Ravoori, W.M. Merritt, Y.G. Lin, L. S. Mangala, T.J. Kim, R.L. Coleman, C.N. Landen, Y. Li, E. Felix, A.M. Sanguino, R.A. Newman, M. Lloyd, D.M. Gershenson, V. Kundra, G. Lopez-Berestein, S. K. Lutgendorf, S.W. Cole, A.K. Sood, Chronic stress promotes tumor growth and angiogenesis in a mouse model of ovarian carcinoma, Nat Med 12 (2006) 939–944, https://doi.org/10.1038/nm1447.

[23] I. Guerriero, H. Ramberg, K. Sagini, M. Ramirez-Garrastacho, K.A. Taskén, A. Llorente, Implication of β2-adrenergic receptor and miR-196a correlation in neurite outgrowth of LNCaP prostate cancer cells, PLoS One 16 (2021), https://doi.org/10.1371/JOURNAL.PONE.0253828.

[24] P. Zhang, X. He, J. Tan, X. Zhou, L. Zou, β-2 adrenergic receptor signaling inducing prostate cancer cell progression, Oncol. Rep. 26 (2011) 1471–1477, https://doi.org/10.3892/or.2011.1417.

[25] L. Brohée, O. Peulen, B. Nusgens, V. Castronovo, M. Thiry, A.C. Colige, C.F. Deroanne, Propranolol sensitizes prostate cancer cells to glucose metabolism inhibition and prevents cancer progression, Sci. Rep. 8 (2018), https://doi.org/10.1038/S41598-018-25340-9.

[26] J. Yang, L. Jia, Q. Hao, Y. Li, Q. Li, Q. Fang, A. Cao, New biodegradable amphiphilic block copolymers of ε-caprolactone and δ-valerolactone catalyzed by novel aluminum metal complexes: II. Micellization and solution to gel transition, Macromol. Biosci. 5 (2005) 896–903, https://doi.org/10.1002/mabi.200500096.

[27] Q.Q. Yin, L.H. Xu, M. Zhang, C. Xu, Muscarinic acetylcholine receptor M1 mediates prostate cancer cell migration and invasion through hedgehog signaling, Asian J. Androl. 20 (2018) 608–614, https://doi.org/10.4103/aja.aja_55_18.

[28] M. Zhang, Q. Wang, X. Sun, Q. Yin, J. Chen, L. Xu, C. Xu, β 2 -adrenergic receptor signaling drives prostate cancer progression by targeting the Sonic hedgehog-Gli1 signaling activation, Prostate 80 (2020) 1328–1340, https://doi.org/10.1002/PROS.24060.

[29] C.L. Buchheit, R.R. Rayavarapu, Z.T. Schafer, The regulation of cancer cell death and metabolism by extracellular matrix attachment, Semin. Cell Dev. Biol. 23 (2012) 402–411, https://doi.org/10.1016/J.SEMCDB.2012.04.007.

[30] P. Wu, M. Cai, J. Liu, X. Wang, Catecholamine surges cause cardiomyocyte necroptosis via a RIPK1–RIPK3-dependent pathway in mice, Front Cardiovasc Med 8 (2021) 740839, https://doi.org/10.3389/FCVM.2021.740839.

[31] L. Sun, H. Wang, Z. Wang, S. He, S. Chen, D. Liao, L. Wang, J. Yan, W. Liu, X. Lei, X. Wang, Mixed lineage kinase domain-like protein mediates necrosis signaling downstream of RIP3 kinase, Cell 148 (2012) 213–227, https://doi.org/10.1016/j.cell.2011.11.031.

[32] X. Liu, X. Xie, Y. Ren, Z. Shao, N. Zhang, L. Li, X. Ding, L. Zhang, The role of necroptosis in disease and treatment, MedComm (Beijing) 2 (2021) 730–755, https://doi.org/10.1002/MCO2.108.

[33] L. Seifert, G. Werba, S. Tiwari, N.N. Giao Ly, S. Alothman, D. Alqunaibit, A. Avanzi, R. Barilla, D. Daley, S.H. Greco, A. Torres-Hernandez, M. Pergamo, A. Ochi, C.P. Zambirinis, M. Pansari, M. Rendon, D. Tippens, M. Hundeyin, V.R. Mani, C. Hajdu, D. Engle, G. Miller, The necrosome promotes pancreatic oncogenesis via CXCL1 and Mincle-induced immune suppression, Nature 532 (2016) 245–249, https://doi.org/10.1038/nature17403.

[34] X. Pan, G. Chen, W. Hu, Piperlongumine increases the sensitivity of bladder cancer to cisplatin by mitochondrial ROS, J. Clin. Lab. Anal. (2022), https://doi.org/10.1002/JCLA.24452.

[35] X. Ji, R. Wang, H. Tang, H. Chen, L. Bao, F. Feng, P. Jia, Necroptosis of osteoblasts was induced by breast cancer cells in vitro, Transl. Cancer Res. 9 (2020) 500–507, https://doi.org/10.21037/TCR.2019.11.32.

[36] L. Liu, J. Fan, G. Ai, J. Liu, N. Luo, C. Li, Z. Cheng, Berberine in combination with cisplatin induces necroptosis and apoptosis in ovarian cancer cells, Biol. Res. 52 (2019) 37, https://doi.org/10.1186/S40659-019-0243-6.

[37] Y. qiang Yu, V. Thonn, J.V. Patankar, O.M. Thoma, M. Waldner, M. Zielinska, L. li Bao, M. Gonzalez-Acera, S. Wallmüller, F.B. Engel, M. Stürzl, M.F. Neurath, E. Liebing, C. Becker, SMYD2 targets RIPK1 and restricts TNF-induced apoptosis and necroptosis to support colon tumor growth, Cell Death Dis. 13 (2022), https://doi.org/10.1038/S41419-021-04483-0.